ELSEVIER

Biochimica et Biophysica Acta 1329 (1997) 51–60

BIOCHIMICA ET BIOPHYSICA ACTA
BBA

The hinge portion of the *S. aureus* α-toxin crosses the lipid bilayer and is part of the *trans*-mouth of the channel

Oleg V. Krasilnikov [a,b,*], Liliya N. Yuldasheva [b,c], Petr G. Merzlyak [a,b], Maria-Fatima P. Capistrano [b], Romildo A. Nogueira [b]

[a] *Laboratory of Molecular Physiology, Institute of Physiology and Biophysics, 700095 Tashkent, Uzbekistan*
[b] *Laboratory of Membrane Biophysics, Department of Biophysics and Radiobiology, Federal University of Pernambuco, 50670-901, Recife, PE, Brazil*
[c] *Department of Biochemistry, Tashkent Pediatric Medical Institute, 700125 Tashkent, Uzbekistan*

Received 3 February 1997; accepted 24 March 1997

Abstract

This paper compares the functional properties of ion channels formed in planar lipid membranes by the wild and mutant *Staphylococcus aureus* α-toxin. It was shown that replacement of the amino acid Gly at position 130 by Cys in the primary structure of the toxin decreases the single-channel conductance with a concomitant decrease in the pH at which the channel becomes unable to discriminate between Cl^- and K^+ ions. The mutation also induced an increase in the asymmetry in the current–voltage relationship of the channel. The results of our experiments suggest that the *trans*-mouth of the channel is responsible for all the observed changes in channel properties. It was assumed that this entrance is built by the glycine-rich hinge portion of the toxin and is situated close to the surface of monolayer facing the *trans*-compartment. © 1997 Elsevier Science B.V.

Keywords: Alpha toxin; Planar lipid bilayer; Ion channel

1. Introduction

α-Hemolysin (ST) is one of the most important toxins produced by *Staphylococcus aureus*. The toxin is a single-chain polypeptide of 33,200 Da (293 amino acids) and is secreted as a water-soluble monomer, which assembles into cylindrical pores in membranes. The secondary structure of both the monomer and oligomer is predominantly a β-sheet. It has been proposed that the toxin undergoes a conformational change during assembly, involving the separation of two rigid domains connected by a glycine-rich loop near the midpoint of the polypeptide chain, converting the molecule into an amphipathic rod, seven [1] of which form a *trans*-membrane pore. A glycine-rich sequence (residues 119–143), thought to be the loop, is susceptible to proteases in the monomer, but not in the oligomer form. It has been demonstrated that almost all biological effects of the toxin are based on its ability to form water-filled pores in target membranes. This toxin is also active

* Corresponding author. Universidade Federal de Pernambuco, Centro de Ciencias Biologicas, Depto. de Biofisica e Radiobiologia, Av. Prof. Moraes Rego, S/N, Cidade Universitaria, Recife, Pernambuco, Brazil, CEP: 50670-901. Fax: (55) (81) 271-8560/2718142; E-mail: kras@npd.ufpe.br

PII S0005-2736(97)00087-4

in planar lipid bilayers as can be deduced from first reports made more than 15 years ago [2,3]. The toxin structure and the structure and properties of the ion channel formed by it have been intensively studied during the last 20 years. However, we are far from understanding the role of individual amino acids on the structure and functions of the ion channel formed by the toxin. To tackle this issue, two groups of investigators started to produce mutant toxins [4–11]. From these studies an assumption was made that a central glycine-rich loop (the so-called 'hinge' region) of the toxin is of little significance for oligomerization in the membrane, but that it can be responsible for the 'correct' structure of the conductive channel. However, the properties of the *trans*-membrane ion channels induced by these mutant toxins in membranes have not yet been investigated. Recently it was shown [12] that using mutant α-toxin having Cys at position 130 of the primary structure of the toxin can be of help in the effort to localize the hinge part of the protein in the channel structure. The authors used liposomes as a model system and *N*-(7-nitrobenz-2-oxa-13-diazol-4-yl)-1,2-bis(hexadecanoyl)-*sn*-glycero-3-phosphoethanolamine as an energy acceptor. They found that the distance between acrylodan (an energy donor, that labeled Cys^{130}) and the inner leaflet of the liposome is short (0.5 ± 0.02 nm).

In this study we incorporated wild and mutant channels into planar lipid bilayers and found that the *trans*-entrance of the α-toxin-formed channel is situated close to the surface of the second leaflet of a bilayer lipid membrane. All differences observed between channels induced by the native and the mutant toxins can be ascribed to changes taking place only at the *trans*-mouth of the channel which comprises the hinge part of the toxin molecule.

2. Materials and methods

2.1. Membranes and electrophysiology

Planar bilayer lipid membranes were formed at room temperature (25 ± 2°C) by the technique of Montal and Mueller [13]. Monolayers were made from a 10-mg/ml solution of lipids in *n*-hexane on the surface of two buffered salt solutions (4 ml) separated by a 25-μm-thick Teflon partition in a Teflon experimental cell. After evaporation of the solvent, the membrane was formed by raising the monolayers above the level of the hole (~ 0.1 mm in diameter) which had been pretreated with a 2% solution of Vaseline in *n*-hexane. Bilayer formation was followed by continuously monitoring the capacitive current in response to a square-wave voltage pulse (amplitude, ± 5–10 mV; frequency, ~ 500 Hz).

Experiments were done under voltage-clamp conditions. The current flowing through the bilayer was measured with Ag/AgCl electrodes connected through salt bridges (3% agar with 3 M KCl) to a voltage source and a current-to-voltage converter. Junction potentials were always around 1 mV and were electronically compensated. The *trans*-compartment of the experimental chamber was connected to the virtual ground while voltage pulses were applied to the *cis*-compartment, defined as the side to which proteins are added. The amplifier signal was monitored with a storage oscilloscope and recorded on a strip chart recorder. The basal conductance of the non-modified PLM was in the range of 4–8 pS. The solutions in both compartments were magnetically stirred. In order to stop channel incorporation, the solution containing the toxin was replaced by fresh buffer.

The selectivity of the ion channels was measured in the presence of a three-fold KCl concentration gradient (300 mM/100 mM KCl, *cis*/*trans*). Zero current potential was defined as the potential (V^*) that must be applied to the experimental cell in order to reach virtual zero current.

Instantaneous current–voltage relationships (CVR), were measured by applying a voltage ramp from -150 to $+150$ mV at a frequency of 5 Hz. Reversing the direction of the ramp did not change the *I*–*V*. The relationship between the current flowing through the channels at -100 mV and at $+100$ mV (I_{-100}/I_{+100}) was taken as a quantitative measure of the asymmetry (A) in the CVR. To evaluate non-linearity in the positive (L_+) and in the negative (L_-) branches of the CVR we used a relation between values of the membrane conductance at 100 mV and at 20 mV ($L_+ = G_{100}/G_{20}$; $L_- = G_{-100}/G_{-20}$).

2.2. Channel-sizing experiments

The maximal radius of the channel was determined according to a method described in [14–16]. Briefly,

non-electrolyte molecules of different hydrodynamic sizes were used to probe the channel structure. Mean single-channel conductances were determined in the presence of 20% (w/v) of one of the test non-electrolytes and used in conjunction with the solution conductivities to calculate a permeability parameter, ν, as follows:

$$\nu = [(G_o - G)/G_o]/[(H_o - H)/H_o] \quad (1)$$

Where H_o and G_o are the electrical conductivity of 0.1 M KCl solution and the single-channel conductance in that same solution, respectively and H and G are the electrical conductivity of 0.1 M KCl solution containing 20% of the test non-electrolyte and the channel conductance in that same solution, respectively.

The maximal radius of the channel was taken to be equal to the minimal hydrodynamic radius of an impermeable non-electrolyte molecule, i.e., a molecule that does not decrease the ion channel conductance at all. In practice, it was determined from the relationship between ν and the hydrodynamic radii of the non-electrolytes. The intercept between the linear portion of that relation and the quasi horizontal portion, where ν does not vary with radii, is taken as the pore size.

2.3. Chemicals

Pure phosphatidylcholine was prepared from fresh egg yolk according to Bergelson et al. [17]. When it was especially noted phosphatidylcholine purchased from Sigma (Type V-E) was used as received. Azolectin (Type II, Sigma) was purified by acetone extraction [18]. Cholesterol and dithiothreitol (DTT) were purchased from Sigma and used as received.

The non-electrolytes glycerol (Sigma); glucose (Merck), polyethylene glycol (PEG) 400 (Sigma), PEG 1000 and PEG 1450 (Sigma), PEG 2000, PEG 3000 and PEG 4000 (Loba Chema), PEG 6000 (Sigma) were used as received or additionally purified by anion-exchange chromatography using strong alkaline anion exchangers (III or IV, Merck) when needed. The hydrodynamic radii of the non-electrolytes were taken from [14–16].

Doubly distilled water was used in the preparation of all buffer solutions. For the bilayer experiments, a standard bathing solution contained: 0.1 M KCl, 0.005 M Tris-OH, and the pH was adjusted to the appropriate value with citric acid. Where noted, this buffer also contained DTT at a final concentration of 1–10 mM. The conductivity of each buffer solution was measured with a multi-range conductivity meter (HANNA Instruments-model HI 9033) at 25°C.

Other chemicals were of analytical grade and were used without additional purification.

Protein concentration was determined with a Bradford reagent (Bio-Rad) using bovine serum albumin as standard.

2.4. Toxins

Both wild (ST) and mutant (MST) α-toxin were donated to us by Prof. S. Bhakdi and Dr. M. Palmer (Institute of Medical Microbiology, University of Mainz, Germany). The mutated toxin contains a cysteine in position 130 instead of the original glycine.

2.5. Statistics

Where pertinent, the data are presented as mean ± S.D. The Student *t*-test was used to evaluate the significance of the difference between mean values.

3. Results and discussion

3.1. MST forms ion channels in lipid bilayers

The addition of MST to a voltage-clamped lipid bilayer results in stepwise increases in current (Fig. 1) with unitary conductance around 20 pS and only a few events exceeding 50 pS. This single-channel conductance is much smaller than that shown by channels formed by the wild toxin, normally in the range of 80–120 pS, as can be seen in Fig. 1. DTT (in 1–10 mM concentration) did not change the distribution of single-channel conductances, suggesting that under our experimental conditions, disulfide bridges are not formed, and MST should exist as monomers in solution.

3.2. The cation–anion selectivity of MST channels

The cation–anion selectivity and the current–voltage relationship (CVR) of the α-toxin channel seem

to be associated with charged residues distributed around the ion channel mouths [14,19]. The native and the mutant toxins differ from each other only by the type of amino acid present at position 130. The substitution of Gly for Cys should induce changes in the local structure of the protein due to the different sizes of the side chains, leading to modifications in the charge distribution around the channel mouths and, therefore, in ion selectivity and/or in the current–voltage relationship of the mutant channel in relation to the wild toxin channel. Since both the selectivity and the current–voltage relationship are determined by charged residues in the protein molecule, it is expected that changes in the pH of the bathing solutions should induce changes on those parameters reflecting the actual charge distribution around the mouth of the channel.

Fig. 2 shows results of this kind of experiment. For pH < 5.7 the reversal potentials (V^*) of channels formed by MST in neutral phosphatidylcholine (PC) bilayers, are positive indicating a higher permeability to chloride than to potassium ions. At pH ≈ 5.7 the channels were not able to discriminate between Cl^- and K^+ ions ($V^* \approx 0$) and for pH > 5.7 the reversal potentials are in the negative region, indicating a higher selective to cations than to anions. Fig. 2 also shows that the pH required for abolishing the selectivity in channels formed by the mutant toxin (~ 5.7) is completely different from the one required by the wild-type toxin (pH ≈ 10).

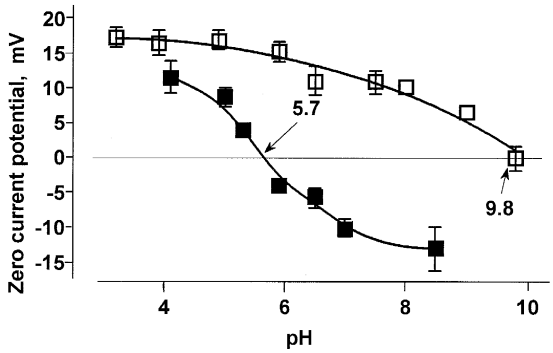

Fig. 2. Effects of pH on the zero current potential. Membranes were formed from a mixture of phosphatidylcholine/cholesterol (3:1; w/w). The toxin was added to the *cis*-compartment at a final concentration equal to 0.5–2.5 μg/ml. A 300 mM/100 mM (*cis*/*trans*) KCl concentration gradient was used. All KCl solutions were buffered with 5 mM citrate-Tris. Values are presented as mean $\pm$ S.D. of 3–7 separate experiments. Where not drawn, the deviation bar was smaller than the symbols used. Lines were fitted by eye. The presence of 1–10 mM DTT in bathing solutions did not change the data. Other experimental conditions are given in Section 2: Materials and methods and in the text. ■, mutant-ST; □, wild toxin.

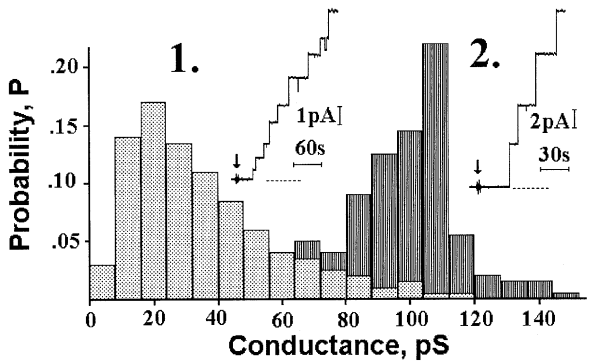

Fig. 1. Amplitude histogram of conductance fluctuations induced by MST (1) and by the wild-type toxin (2). Membranes were made from a mixture of phosphatidylcholine/cholesterol (1:1, w/w) and voltage-clamped at -50 mV. P is the probability to observe steps in channel conductance in a current vs. time record; bin width is 8 pS. More than 800 and 200 events were measured (5–7 channels in each membrane) for MST and for wild-type toxin, respectively. The record was stopped if any of the open channels temporarily closed. Inserts show the original single-channel recordings. The dashed line indicates zero current, while arrows indicate additions of the toxin (1–2 nM). Bathing solutions contained 100 mM KCl, 5 mM Tris-citrate, pH 7.5. In separate experiments, DTT was added to the bathing solution (1–10 mM final concentrations) before the addition of MST and this changes neither the conductance nor other properties of the MST channels.

The above results can be interpreted by assuming that the cation–anion selectivity of large water-filled channels can be described by the sum of the effective electrical potentials contributed by the ionogenic (titratable) groups present in the proximity of both channel entrances [14,19]. The individual contribution of each group is dependent on the distance between this group and the central region of the channel entrance. This same type of phenomenon should be responsible for the asymmetry observed in the current–voltage relationship: it could be described through the ratio of the effective electrical potentials at the channel entrances.

Taking the above argument into account and the measured values of the cation–anion selectivity of

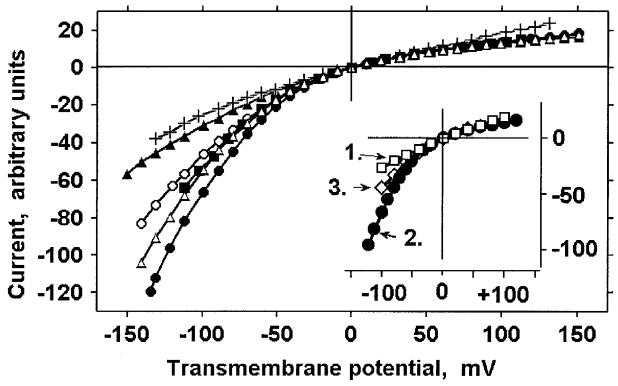

Fig. 3. Current–voltage characteristics of channels formed by the mutant ST. Membranes were formed from a mixture of phosphatidylcholine/cholesterol (3:1; w/w). If not mentioned, buffer 1 was used with the appropriate pH. MST (in the concentration range of 0.01–2.5 μg/ml) was added on the *cis*-side. After the conductance reached a quasi steady-state value, CVR was measured according to the voltage protocol described in Section 2: Materials and methods. The results are from separate experiments. Symbols at 100 mM KCl: ■, pH 9.0; △, pH 8.0; ●, pH 7.0; ○, pH 5.0; ▲, pH 4.0; and +, 3.0 M KCl, pH 8.0. Insert: Current–voltage relationships of: 1, wild ST formed channel in PC-bilayers; 2, mutant-ST-formed channel in PC-bilayers; and 3, wild ST-formed channel in PC/Az (*cis/trans*) bilayers. Solution containing 100 mM KCl and pH 7.5 was used in all these cases. Current scale is in arbitrary units.

MST and ST channels, we can conclude that the distribution of titratable charges around the ion channel mouths is altered when Gly is substituted for Cys at position 130. Moreover, we can assume that titratable groups which are able to generate negative potentials are more important in determining the selectivity of MST channels than of the wild-type ST channels.

3.3. The current–voltage relationships

To further look for the presence of titratable groups in the toxin channel, we have measured the *I–V* characteristics as a function of pH and lipid charge. The results are shown in Fig. 3. As can be seen, the CVR of the MST channels was drastically different from that of wild ST channels in the sense that it exhibits a more pronounced non-linearity and asymmetry. Increasing the electrolyte concentration in the bathing solutions transformed this CVR to a more symmetrical and linear shape (+ symbol in Fig. 3). This result is indicative that the main energetic barrier(s) for passing ions through the MST channel water lumen is actually determined by the titratable charged residues. Another point of interest is that the asymmetry in the *I–V* curves, evaluated through the parameter *A*, is dependent on the pH of the solutions, but this dependence is completely distinct for MST and wild ST channels, as shown in Fig. 4. The parameter *A* was relatively small at pH 4.0 (2.4 ± 0.1; $n = 5$), increasing with pH to a maximum of 4.9 ± 0.5 ($n = 7$) at pH 7.0, and then slightly decreasing with further increases in pH, not following a simple titration curve. This fact can be taken as an indication that the effects of the mutation are not directly associated with ionization of the thiol group of the Cys^{130} residue. In comparison with these results, the values of *A* for the wild type toxin are 1.0 ± 0.2 ($n = 4$) at

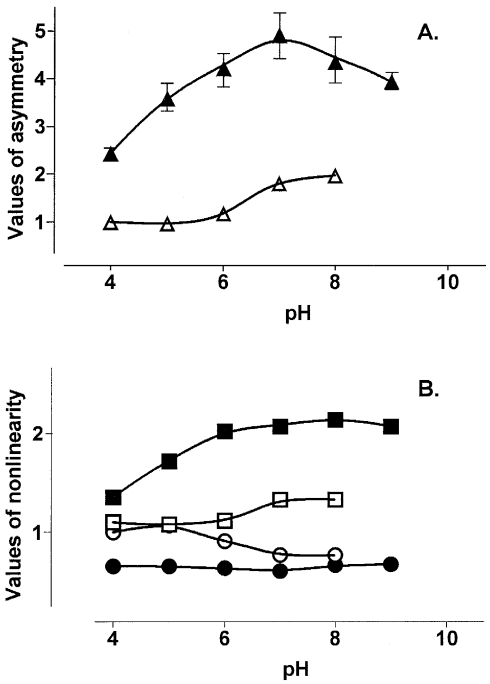

Fig. 4. pH-dependencies of the asymmetry (A) and non-linearity (B) parameters. ▲ and △, asymmetry for membranes modified by the mutant and wild ST, respectively; ● and ○, non-linearities at positive potentials; ■ and □, non-linearities at negative potentials; open symbols refer to wild-type toxin and closed symbols to the mutant. Values are presented as mean ± S.D. of 4–10 separate experiments. Where not drawn, the deviation bar was smaller than the symbols used. The lines were drawn by eye. Buffer 1 was used with the appropriate pH. Other experimental conditions are given in Section 2: Materials and methods and in the text.

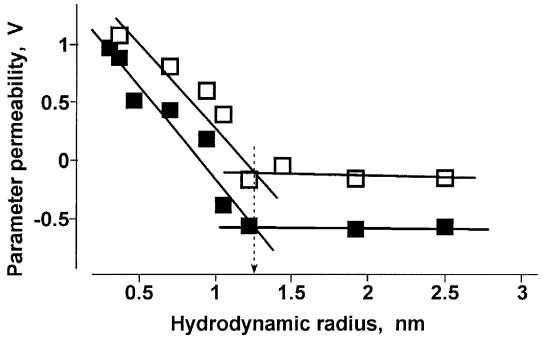

Fig. 5. Dependence of the parameter ν on the hydrodynamic radii of non-electrolytes. Symbols: ■, MST-channels; □, wild ST channels (data taken from [19]). Buffer 1 (with pH 7.5) and buffer 1 containing 20% of the appropriate non-electrolyte were used. The hydrodynamic radii of non-electrolytes which were taken from [14–16] and were the following: 0.31 ± 0.02 nm for glycerin, 0.37 ± 0.02 nm for glucose, 0.47 ± 0.02 nm for sucrose, 0.7 ± 0.03 nm for PEG 400, 0.94 ± 0.04 nm for PEG 1000, 1.05 ± 0.04 nm for PEG 1450, 1.22 ± 0.04 nm for PEG 2000, 1.44 ± 0.04 nm for PEG 3000, 1.92 ± 0.03 nm for PEG 4000, and 2.5 ± 0.03 nm for PEG 6000. More than 200 current transition were registered (5–9 channels per membrane) for each experimental condition. Arrow indicates the maximal values of the radii of the water pores. All other experimental conditions are as described in the legend to Fig. 1 and in the text and in Section 2: Materials and methods.

pH 4.0 and 1.8 ± 0.2 ($n = 5$) at pH 7.0 indicating that the ionogenic groups are much more asymmetrically distributed between the two entrances of the channel formed by the mutant toxin than by the wild type.

3.4. The size of MST-induced water pore in planar lipid bilayer membranes

Since we are assuming that the mutation has induced a rearrangement in the local structure of the protein, leading to a redistribution of charges at the channel mouths, we also decided to investigate whether such changes have modified the diameter of the ion channel. The experiments were made as describe in methods to evaluate the permeability parameter, ν, as a function of the non-electrolyte radii. The results are shown in Fig. 5 and indicate that the maximal radius of the water pore formed by MST has the same value as that of the pore formed by the wild-type toxin, and equal to 1.2–1.3 nm.

The data so far described allow us to conclude that the smaller single-channel conductance observed for MST, in comparison with that of wild ST, does not result from a decrease in the channel diameter. Instead, this last result reinforces the hypothesis that the smaller conductance of the MT channel is determined by a new distribution of titratable negative groups around the channel entrances.

3.5. Orientation of the MST in the membrane

Assuming that the selectivity of MST channels (as that of wild ST channels [14,19]) is determined by charged groups and sensitive to the surface potential

Table 1
Effect of the lipid composition on the zero current potential (mV) of mutant and wild ST induced ion channels in bilayer lipid membranes

KCl	Lipid composition (*cis*/*trans*)			
(*cis*/*trans*; mM)	PC/PC	Az/Az	PC/Az	Az/PC
Mutant ST				
300/100	-5.6 ± 1.6 [a] (5)	-14.0 ± 0.5 (5)	-12.8 ± 1.3 (7)	-6.4 ± 0.6 [a] (7)
100/300	0.4 ± 1.0 [a] (5)	1.1 ± 0.7 [a] (7)		
Wild ST				
300/100	11.8 ± 1.4 (7)	5.9 ± 0.5 [a] (6)	6.2 ± 1.0 [a] (6)	9.5 ± 0.6 (6)
100/300	-8.0 ± 0.8 [a] (7)	-7.3 ± 0.4 [a] (5)		

The bilayers were formed by the apposition of two monolayers with the lipid composition noted in the table. Zero current potential was measured in the presence of a three-fold *trans*-membrane KCl gradient as indicated. Values of zero current potential are reported as mean ± S.D. The number of experiments is given in parentheses; each measurement was obtained from a different membrane. For 300/100 mM KCl gradient, negative values denote a preference for potassium ion and positive values denote a preference for chloride. For 100/300 mM KCl gradient, negative values denote a preference for chloride ion and positive values denote a preference for potassium. All solutions contained 5 mM citric acid and were adjusted to pH 6.5 by Tris-OH. The addition of 1–10 mM DTT to the bathing solutions did not change the data. Other conditions of the experiment are the same as described in the text.
[a] $P > 0.03$.

we designed experiments to test for the orientation of the protein in the membrane. To this end, membranes were formed by the apposition of two different monolayers, one made with a neutral lipid such as PC and the other with azolectin (Az), known to contain negatively charged lipids. The toxin was applied to the *cis*-side of the PLM and then the zero current potential was measured in the presence of an 3:1 ion gradient. The results of this set of experiments are presented in Table 1.

When the toxin was added to the solution facing the PC monolayer, of a PC/Az PLM, the reversal potential was not different from that observed in a pure azolectin (Az/Az) PLM. On other hand, addition of the toxin to the azolectin side of an Az/PC membrane results in a zero current potential not different from that observed for a pure PC (PC/PC) PLM. This implies that the entrances of the channel are at different distances from the polar head groups of the membrane lipids. If we call the channel entrance which protrudes from the plane of the membrane into the side to which the toxin was added the '*cis*'-entrance and the other side the '*trans*'-entrance of the channel, then we can conclude that the '*cis*'-entrance is placed farther from the surface of the polar lipid head groups than the '*trans*'-entrance. It is worth noting that ion channels formed by the wild ST [11,14,19] have the same orientation in the membrane plane as the MT channels. It is suggesting that the point mutation does not change the protein insertion and orientation in the PLM. Increasing the KCl concentration from 100 mM (Debye length ~ 0.97 nm) to 300 mM (Debye length ~ 0.56 nm), on the *trans*-side of PLM, induced an almost complete screening of the negatively charged lipids. This fact is suggested because the reversal potentials measured both in a PC and an Az bilayer became practically the same (Table 1). These results indicate that the distance between the *trans*-entrance of MST and the polar heads of the lipid is actually short.

3.6. The structural differences between the wild and mutated channels

As shown in the insert to Fig. 3, the CVR of wild-ST channels can be transformed to a sharply asymmetrical and non-linear relation, as long as, a negative surface potential exists at the *trans*-surface of the bilayer. This observation confirms the important role of the negative charges generated by titratable groups in determining MST channel properties. In addition it also shows that these changes have to be localized mainly at the *trans*-entrance of the channel.

From a theoretical point of view (see Appendix A) the system can be described by assuming that the addition of about 11 negative charges to the *trans*-entrance of the wild ST channel is sufficient to adequately transform its properties into that typical of the MST channel, at pH 7.0. This kind of reasoning

Table 2
Parameters of the current–voltage characteristics in symmetrical and asymmetrical pH conditions

CVR parameters	pH [a] (*cis*/*trans*)			
	8.0/8.0	5.0/5.0	8.0/5.0	5.0/8.0
Mutant ST				
A	4.4 ± 0.5 (7)	2.1 ± 0.2 (3)	1.9 ± 0.1 (5)	5.3 ± 0.4 (5)
L_-	1.9 ± 0.1 (7)	1.3 ± 0.2 (3)	1.3 ± 0.1 (5)	2.2 ± 0.2 (5)
L_+	0.6 ± 0.1 (7)	0.7 ± 0.1 (3)	0.8 ± 0.1 (5)	0.6 ± 0.1 (5)
Wild ST				
A	2.0 ± 0.2 (3)	1.0 ± 0.1 (3)	0.6 ± 0.1 (4)	2.3 ± 0.1 (4)
L_-	1.4 ± 0.1 (3)	1.1 ± 0.1 (3)	0.8 ± 0.1 (4)	1.5 ± 0.1 (4)
L_+	0.8 ± 0.1 (3)	1.1 ± 0.1 (3)	1.2 ± 0.1 (4)	0.8 ± 0.1 (4)

The bathing solutions were 100 mM KCl plus 5 mM K-phosphate buffer. pH was adjusted to the appropriate value by additions of small aliquots of 1 M KOH and 1 M citric acid. The membrane was formed from a mixture of phosphatidylcholine (Sigma)/cholesterol (3:1, w/w). Values are reported as mean $\pm$ S.D. The number of experiments is given in parentheses; each measurement was obtained from a different membrane.

[a] pH refers to the value at the beginning of the experiment.

also shows that the presence of seven thiol groups in a heptamer ST channel [1] are not a sufficient condition to determine the observed increment in negative charges at the *trans*-entrance. Therefore we have to assume that other amino acid residues which can contribute a net negative charge should be situated closer to the *trans*-entrance in the structure of the mutated- than in that of the wild-type channels. These charges could be ascribed to Asp^{127} and Asp^{128} residues, for example.

3.7. The pH-sensitive mouth of the channel

The pH dependence of the CVR non-linearity, shown in Fig. 4B, can be viewed as another possibility to clarify the structural features of the channels. In this way, the parameter L_+ was weakly pH-depend whereas L_- was strongly pH-dependent. Like that the differences in CVR between the ST and MST channels are mainly determined by differences in L_-.

For the localization of the 'pH-sensitive mouth' of the channel the experiments in which the pH was changed in only one side of the bilayer were designed. It was found that a decrease in the pH, from 8.0 to 5.0, on the *cis*-side of the PLM changed neither the asymmetry nor the non-linearity of CVR, significantly (Table 2). On the contrary, both parameters were slightly increased. However, analogous changes in the pH of the *trans*-side of the bilayer sharply modified the CVR shape. It became practically equal to that of a membrane in which the pH was simultaneously decreased to 5.0 on both of its sides. Very similar results were obtained for a PLM modified by the wild type toxin. The differences between the CVR parameters obtained at 5.0/5.0 and 8.0/5.0 or between those obtained at 8.0/8.0 and 5.0/8.0 were not large. Hence, the *trans*-entrance of MST and wild ST channels are much more pH-sensitive than the *cis*-one and structural differences in the *trans*-entrances of these channels should be the main cause of the differences in their CVRs.

The above assumption is also supported by data derived from the electrostatic model [14,19] outlined in the appendix. It was found that the pH-dependencies of calculated effective charges at the *cis*-entrance of the channels are quite the same (Fig. 6A) while the pH dependent of the *trans*-entrance effective charge is much larger for the MST channel than for the wild-type (Fig. 6B). These dependencies are basic for, and can explain the observed pH effects on, the cation–anion selectivity and CVR parameters of the wild and the mutated channels. Since the number of effective charges on the *trans*-side of the mutated and the wild-type ST heptamerical channels is considerably larger than 7 (11–12 in the pH range 6.0–9.0; Fig. 6) we are forced to assume that some other carboxyl-containing side chain, neighboring Cys^{130}, must be part of the total *trans*-entrance charge. This assumption is valid even if the SH group of Cys^{130} takes part in the process. We do not have an exact idea about the amino acid residues responsible for this effect but Asp^{127} and Asp^{128} are close to position 130 and could contribute to this end.

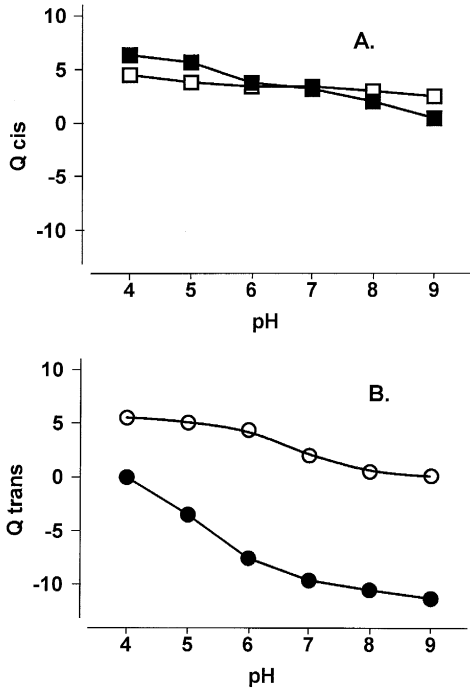

Fig. 6. pH-dependencies of the effective charge at the *cis*-entrance (A) and *trans*-entrance (B) of the channel formed by wild-type (open symbols) and mutant ST (closed symbols). The values of the effective charge were established by computer simulation of the mathematical model of the channel as described in Appendix A.

The contribution of Cys^{130} to the total charge can be ruled out based on our direct experiments with SH-specific reagents (like NMM, DTNB and IAA). Using planar lipid bilayers, we found that the reagents did not change the cation–anion selectivity and CVR

asymmetry of preformed MST channels (data not shown). Hence SH group of Cys^{130} is not available to the reagents in the heptameric channel structure and not contacted with water solution. Latter conclusion is reinforced by the experiments with the toxin site-specifically labeled with acrylodan, a polar sensitive probe [20], which suggest that the 130th amino acid residue (as many other residues at 126–140 zone of ST) is at hydrophobic environment in the channel structure.

As noted above, it is most likely that the differences in structures between the ST and MST molecules are localized around Cys^{130} both in monomers and in all subunits of the channel inserted into the membrane. Then, localizing the sites responsible for the changes observed in the channel functioning and structure should be equivalent to the determination of Cys^{130} localization. If this assumption holds and since the main differences between ST and MST channels were found to be at the *trans*-entrance of the channels, we have to conclude that the Cys^{130} glycine-rich region of the toxin takes part in the formation of the *trans*-entrance of the oligomeric channel. This portion is known as the hinge.

Our data are in a good agreement with recently published molecular architecture of ST pores [21]. The authors have demonstrated that the glycine-rich part of ST forms two β-strands which contribute to the formation of the *trans*-entrance in the heptameric ion channel structure. Moreover, they predicted that the ends of these β-strands pass through the hydrophobic zone of the membranes and are located close to the second leaflet of the lipid bilayer. The size of the both entrances of the channel calculated by these authors ($\sim$ 2.8 nm at *cis*-entrance (side of protein addition) and $\sim$ 2.4–2.6 nm at *trans*-entrance in diameter) is quite equal to the maximal size of the channel determined by us in planar lipid bilayer experiments (2.4–2.6 nm, Fig. 5 in this article).

4. Conclusion

The data shown in this paper point out that the hinge portion of the toxin (where Cys was introduced) goes through the lipid bilayer and takes part in the formation of the *trans*-mouth of the channel. This entrance of the ST-induced channel is the site sensitive to the charges of the polar head groups of the membrane lipids and might be situated closer to the lipid polar heads than the *cis*-entrance.

Acknowledgements

We are grateful to Prof. S. Bhakdi and Dr. M. Palmer (Institute of Medical Microbiology, University of Mainz, Germany) for providing us with the protein samples. We are grateful to Prof. Wamberto A. Varanda (Department of Physiology, Faculty of Medicine of Ribeirão Preto, University of São Paulo, SP, Brazil) for helpful comments on manuscript preparation. This work was supported by CNPq (Brazil), CAPES (Brazil) and FACEPE (PE, Brazil).

Appendix A

In describing the properties of ST channels we used an electrostatic model published elsewhere [14,19]. In short, the ion transport through the ST channels was assumed to be the effect of the ion's interaction with fixed charges at the channel entrances and following diffusion and migration ions through an asymmetrically charged water pore. For an arbitrary profile of potential energy in a membrane and equilibrium at the channel entrances, the partial current density should be given by [22]:

$$I_i = Z_i \lambda_i RT/F \left[C_i^1 \exp(Z_i \psi) - C_i^2 \right] / \int_o^\delta \exp\left[Z_i \psi (1 - X/\delta) + W_i \right] dx \qquad \text{(A1)}$$

where Z_i is the charge of ion i; λ_i is the equivalent electrical conductance; δ is the channel length; X is the channel length coordinate taken as zero at the *trans*-entrance of the channel and δ at the *cis* one; W_i is the potential energy of the ion in the pore, in kT; $\Psi = \Psi_o + \varphi_1 - \varphi_2$ is the membrane potential difference, in terms of kT/e; C_i^1 and C_i^2 are the equilibrium ion activities at the *cis*- and *trans*-entrances, respectively and connected to the ion activity in bulk solution, C_o, by a Boltzman relationship:

$$C_i = C_o \exp(-Z_i \varphi_i) \qquad \text{(A2)}$$

where

$$\varphi_i = e\,Q_i \exp(-r/L_D) \quad \text{(A3)}$$

is the equivalent potential generated by the titratable charges at the channel entrances; Q_i is the total charge at the respective entrance; r is the channel radius; L_D is Debye length equal to

$$L_D = 1/\left(F\sqrt{(\epsilon\,\epsilon_o\,RT/2C_o)}\right) \quad \text{(A4)}$$

e, π, ϵ, ϵ_o, T, R, F and k have their usual meanings.

Considering the interactions of ions with charges at the channel entrances, the potential energy profile may be expressed as:

$$W_i = Z_i\,\varphi_1 \exp\left[(X-\delta)/L_D\right] + Z_i\,\varphi_2 \exp(-X/L_D) + E. \quad \text{(A5)}$$

The term E has to be included due to several reasons. First, ions in the channel are subject to the action of image forces [22,23]. Moreover, hindrance to the ion movement due to friction forces should also be considered [24]. The principal peculiarity of the latter forces is their independence on the charge sign of the penetrating ions. For simplicity X-independent E was taken as a first approximation. The total current is the product of the sum of the partial currents and the square of the radius and given by:

$$I = \pi\,r^2 \sum I_i. \quad \text{(A6)}$$

In comparing different channels, the values of 1.3 and 10 nm were taken for the radius and length, respectively. Q_1, Q_2 and E were unknown parameters and were obtained from the experimental values of CVR and zero current potentials. Parametrization was carried out by the least square method using a minimum random search algorithm [25]. Confidence intervals for the parameters were found using the Monte-Carlo method. The integral in Eq. (A5) was obtained numerically by the trapezium formula.

References

[1] J.E. Gouaux, O. Braha, M.R. Hobaugh, L. Song, S. Cheley, C. Shustak, H. Bayley, Proc. Natl. Acad. Sci. USA 91 (1994) 12828–12831.
[2] O.V. Krasilnikov, V.I. Ternovsky, Yu.M. Musaev, B.A. Tashmukhamedov, Dokl. Acad. Sci. UzSSR 7 (1980) 66–68.
[3] O.V. Krasilnikov, V.I. Ternovsky, B.A. Tashmukhamedov, Biofisica 26 (1981) 271–275.
[4] M. Palmer, R. Jursch, U. Weller, A. Valeva, K. Hilgert, M. Kehoe, S. Bhakdi, Med. Microbiol. Immunol. 182 (1993) 207.
[5] M. Palmer, R. Jursch, U. Weller, A. Valeva, K. Hilgert, M. Kehoe, S. Bhakdi, J. Biol. Chem. 268 (1993) 11959–11962.
[6] M. Palmer, U. Weller, M. Messner, S. Bhakdi, J. Biol. Chem. 268 (1993) 11963–11967.
[7] B. Walker, M. Krishnasastry, L. Zorn, H. Bayley, J. Biol. Chem. 267 (1992) 21782–21786.
[8] B. Walker, M. Krishnasastry, H. Bayley, J. Biol. Chem. 268 (1993) 5285–5292.
[9] B. Walker, H. Bayley, Protein Eng. 7 (1994) 91–97.
[10] A. Valeva, I. Walev, M. Pinkermell, H. Bayley, M. Palmer, S. Bhakdi, Med. Microbiol. Immunol. 185 (1996) 119.
[11] J.E. Gouaux, L. Song, M.R. Hobaugh, N.T. Southal, J.J. Johnson, Med. Microbiol. Immunol. 185 (1996) 109.
[12] R.J. Ward, M. Palmer, K. Leonard, S. Bhakdi, Biochemistry 33 (1994) 7477–7484.
[13] M. Montal, P. Mueller, Proc. Natl. Acad. Sci., USA 69 (1972) 3561–3566.
[14] O.V. Krasilnikov, R.Z. Sabirov, V.I. Ternovsky, in: B.A. Tashmukhamedov (Ed.), Proteins, Ion Channels and Regulation of Ion Transport through Membranes, FAN, Tashkent, 1991, p. 208.
[15] O.V. Krasilnikov, R.Z. Sabirov, V.I. Ternovsky, P.G. Merzliak, J.N. Muratkhodjaev, FEMS Microbiol. Immunol. 105 (1992) 93–100.
[16] R.Z. Sabirov, O.V. Krasilnikov, V.I. Ternovsky, P.G. Merzliak, Gen. Physiol. Biophys. 12 (1993) 95–111.
[17] L.D. Bergelson, E.V. Dyatlovitskaya, J.G. Molotkovsky, S.G. Batrakov, L.I. Barsukov, N.V. Prokazova, in: Preparative Biochemistry of Lipids, Nauka, Moscow, 1981, pp. 105 and 155.
[18] Y. Kagawa, E. Racker, J. Biol. Chem. 246 (1971) 5477–5487.
[19] O.V. Krasilnikov, R.Z. Sabirov, Gen. Physiol. Biophys. 8 (1989) 213–222.
[20] A. Valeva, A. Weisser, B. Walker, M. Kehoe, H. Bayley, S. Bhakdi, M. Palmer, EMBO J. 15 (1996) 1857–1864.
[21] L. Song, M.R. Hobaugh, C. Shustak, S. Cheley, H. Bayley, J.E. Gouaux, Science 274 (1996) 1859–1866.
[22] V.S. Markin, Yu.A. Chizmadjev, in: Yu.A. Ovchinnikov (Ed.), Induced Ion Transport, Nauka, Moscow, 1974, p. 251.
[23] V.L. Sizonenko, Biofizika 40 (1995) 1251–1255.
[24] V.F. Antonov, Lipids and Ion Permeability of Membranes, Nauka, Moscow, 1982, p. 148.
[25] H. Eler, Statistical Method for Approaching. AINP Report, P11-6816, Dubna, 1972, p. 27, .